Long Duration Assessment of Electron Backstreaming for Ion Optics

IEPC-2009-164

Presented at the 31st International Electric Propulsion Conference,
University of Michigan • Ann Arbor, Michigan • USA
September 20 – 24, 2009

Richard E. Wirz[1]
University of California, Los Angeles, CA, 90095, USA

Abstract: CEX2D-tebs, a new variant of CEX2D, combines electron backstreaming determination and grid erosion into a single model that can assess the long term life and performance of ion optics. The new electron backstreaming technique used in CEX2D-tebs finds the current of high energy electrons that backstream through an ion optics assembly by integrating the random flux of these electrons across the minimum potential surface established by the accel grid. Results show that this technique provides useful and accurate assessments of long duration electron backstreaming for ion optics. The CEX2D-tebs model agrees well with $|V_{ebs}|$ data from the long duration NSTAR tests, LDT and ELT. The best agreement for both the LDT and ELT was found using an initial grid gap slightly larger than that measured in experimental test. The results show that decreasing grid gap over the life of the thruster has a significant effect on the steep rises in $|V_{ebs}|$ observed during the NSTAR ELT. Improved agreement with the ELT results is also found by including the effects of increasing center beamlet current with time, as observed during thruster testing.

Nomenclature

$\bar{c}$	=	average thermal speed
e	=	electron charge
f_{ebs}	=	electron backstreaming fraction
I_{ebs}	=	electron backstreaming current
I_i	=	ion current
m_e	=	mass of electron
n_{bp}	=	average downstream beamlet plasma density
r	=	radius
T_e	=	electron temperature
$\|V_{ebs}\|$	=	electron backstreaming voltage (limit)
ϕ	=	local potential
ϕ_{bp}	=	beam potential
ϕ_m	=	minimum potential along for a radial distance from beamlet axis
Γ_e	=	electron flux

[1] Assistant Professor, Mechanical and Aerospace Engineering, wirz@ucla.edu.

I. Introduction

Excessive electron backstreaming through ion optics can end the effective life of an ion thruster, thus limiting the total ΔV achievable for a mission. Electron backstreaming (EBS) is caused by the random flux of high energy electrons from the thruster's beam that flow back into the discharge chamber by exceeding the potential barrier established by the accel grid. A schematic of this potential barrier is shown in Figure 1, which shows approximate axial potential traces at differing radial positions in the beamlet. It is important to minimize this effect since excessive backstreaming wastes valuable spacecraft power; therefore an electron backstreaming fraction, f_{ebs}, limit of 1% is typically used for ion thrusters [refer to equation (5) below]. The minimum accel grid voltage required to keep f_{ebs} below 1% is called the electron backstreaming voltage (or "limit"), $|V_{ebs}|$. For this condition, the Deep Space One (DS-1) flight spare ion thruster used for the extended life test (ELT) lost the ability to run at full power (TH15) after processing 211 kg of xenon propellant due to $|V_{ebs}|$ values that exceeded the capability of the accel grid power supply [1]. A similar trend of increasing $|V_{ebs}|$ over time was observed during the original NSTAR 8200-hour Long Duration Test [2].

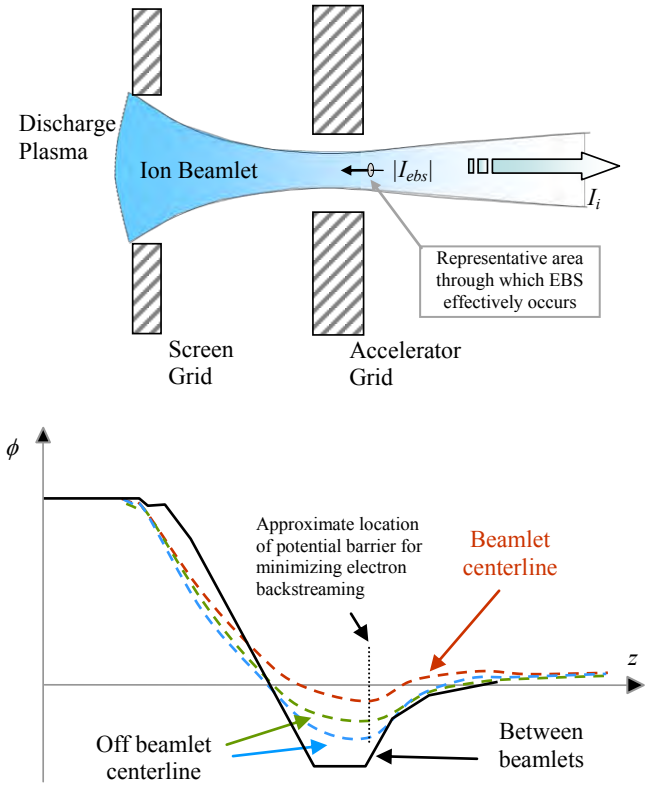

Figure 1. Schematic of an ion beamlet showing approximate potentials at different radial positions from beamlet axis and the small area through which electron backstreaming occurs.

As discussed in reference [3], electron backstreaming can be found computationally by integrating the flow of high energy electrons over the locus of minimum potentials near the downstream end of the accel grid. For individual beamlets it was found that over 99% of the electron backstreaming occurs in a small area at the center of the beamlet that is less than 20% the area of the beamlet is typically located just upstream of the accel grid, as shown schematically in Figure 1. Initial validation against ELT data shows that this technique provides the correct behavior and magnitude of electron backstreaming limit, $|V_{ebs}|$. The results of this study also showed that accel grid chamfering, grid gap change, and screen grid erosion are important to the increase in electron backstreaming observed during the ELT. Therefore, the accurate prediction of thruster life requires time-dependent erosion estimates for the ion optics assembly. As detailed in reference [5], the two-dimensional ion optics code, CEX2D [4], was modified to handle time-dependent erosion, double ions, and multiple throttle conditions in a single run.

The modified code is called "CEX2D-t". Comparisons of CEX2D-t results with the NSTAR thruster life demonstration test (LDT) and extended life test (ELT) results show good agreement for both screen and accel grid erosion including important erosion features such as chamfering of the downstream end of the accelerator grid and reduced rate of accelerator grid aperture enlargement with time. Additionally, the influence of double ions on grid erosion proved to be important for predicting the erosion observed during the LDT and ELT.

In these previous efforts, the method for determining electron backstreaming was validated by using computational formulations external to the CEX2D-t program [3,5]. In this way, CEX2D-t was used to determine the eroded grid geometry and then an external electron backstreaming model was used to estimate f_{ebs} and $|V_{ebs}|$ for a given geometry. The objective of the research presented here is to develop an integrated computational method for determining electron backstreaming for ion optics over long durations. This technique uses time dependent changes in important ion optics features, including: eroded grid geometry, grid gap, grid potentials, and other operating conditions and grid parameters.

II. Technique and Formulation

This section describes a new model called "CEX2D-tebs" that combines grid erosion and $|V_{ebs}|$ determination to produce long-duration assessments of ion thruster life. The $|V_{ebs}|$ determination technique described in this section can be used with any ion optics code that resolves the potential field along the beamlet. This study combines this technique with an improved version of the CEX2D-t code. As discussed above and in reference [5], CEX2D-t develops time dependent eroded geometries of ion optics and uses the popular CEX2D code. The improved version of the CEX2D-t code used in this effort also allows the grid gap of the eroded geometry to change with time, which has been witnessed in experimental tests [6,7].

A flow chart showing the interrelationship of the different components of the model is shown in Figure 2. The model is arranged such that simulations of ion optics erosion progress until a prescribed time, say "t_i", to find how the erosion of the grids will lead to modifications of the grid geometry. If a computational cell of grid material is completely eroded away, then it is considered that the grid geometry has effectively changed. At this point, the code then decides if sufficient time has passed (Δt_{min}) to execute a search for the EBS limit. A minimum time step for performing EBS limit, Δt_{min}, is used to prevent excessive runtimes for higher resolution runs, where the grid geometry can change frequently by small amounts. The code also checks to see if the stop time, t_i, has been reached; if so, the code progresses to the next thruster operating condition specified in "Input ($i+1$)"(at which time, an EBS limit determination is also conducted). At the next operating condition, the model uses the eroded grid geometry but can apply new values for parameters such as grid gap, beamlet current, grid voltages, etc. The technique for determining $|V_{ebs}|$ is giving below.

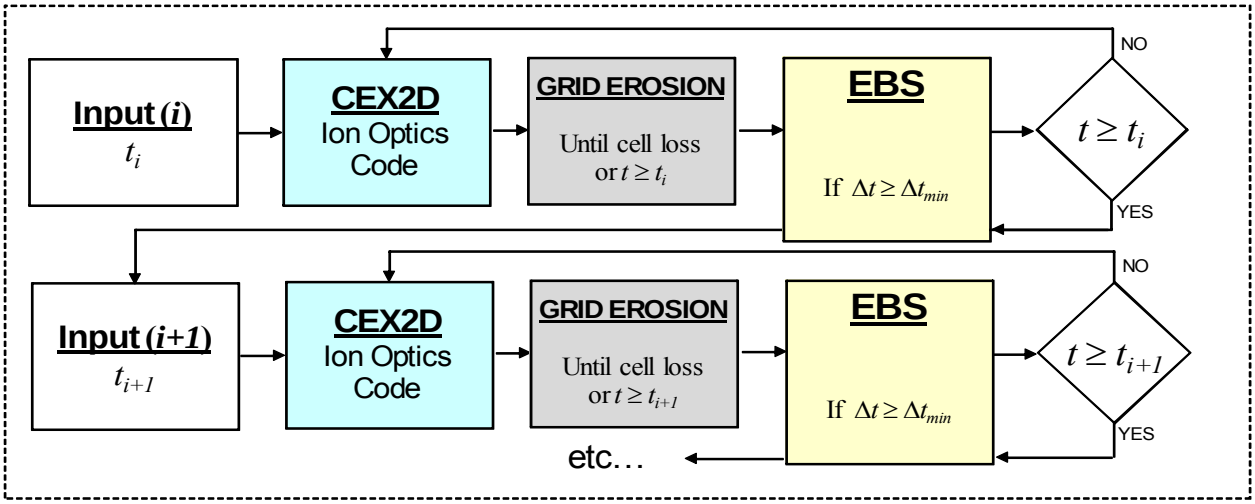

Figure 2. Flow Chart for CEX2D-tebs, showing how electron backstreaming is determined for eroded geometries during long duration analysis of ion optics operation.

The following derivation shows how the electron backstreaming (EBS) current for a single beamlet is determined and then how this current is compared to the beamlet current to find the EBS limit. As discussed in reference [3], electron backstreaming is caused by the random flux of high energy electrons past the potential barrier established by the accel grid. The high energy electrons come from the tail of the thermal distribution of beam electrons. The retarding potential for each radial location for the gridlet (the minimum potential measured along the direction of the beamlet axis) occur near the accel grid aperture in the beamlet, resulting in a small area (pictured in Figure 1) in the center of the beamlet through which higher energy electrons can make their way back into the discharge chamber [3]. The electron backstreaming estimation method developed here assumes the electrons are nearly in thermal equilibrium; in addition the electron drift, inertial, magnetic, and frictional forces are negligible such that the electron density, n_e, at a local potential, ϕ, is described by Boltzmann's relation

$$n_e(\phi) = n_{bp} \exp\left[\frac{\phi - \phi_{bp}}{T_e}\right] \tag{1}$$

where n_{bp}, is the average downstream beamlet density at the beam potential, ϕ_{bp}.

For ion thrusters, the accel grid sets up a potential barrier in the beamlet to prevent backstreaming of beam electrons. The flux of backstreaming electrons from the beam that will make it across a local potential minimum, ϕ_m, and back into the discharge chamber can be determined by using the Boltzmann relation from Equation (1). Since this relation determines the electron densities at local potentials as a function of the downstream beam plasma potential, ϕ_{bp}, and the beam plasma density, n_{bp}, the one-sided thermal flux of electrons for a local potential minimum, ϕ_m, can be expressed as

$$\Gamma_e(\phi_m) = \left(\frac{n_{bp}\bar{c}}{4}\right)\exp\left[\frac{\phi_m - \phi_{bp}}{T_e}\right] \tag{2}$$

where $\bar{c}$ is the average thermal speed of the beam plasma electrons at temperature T_e, measured in the downstream field, and is given by

$$\bar{c} = \sqrt{\frac{8eT_e}{\pi m_e}} \tag{3}$$

The locus of minimum potentials created by the accel grid is found by searching along the beam axis at each radial location in the computational domain. The electron backstreaming current, I_{ebs}, for a gridlet is found by integrating the electron backstreaming flux over the surface defined by local minimum potentials, ϕ_m, such that

$$I_{ebs} = e\iint_S \Gamma_e dS = e\left(\frac{n_{bp}\bar{c}}{4}\right)\iint_S \exp\left[\frac{\phi_m - \phi_{bp}}{T_e}\right] dS \tag{4}$$

The parameters (i.e., n_{bp}, ϕ_{bp}, $\bar{c}$, and T_e) reflect downstream beam plasma conditions and are therefore constant across the integration surface.

The backstreaming fraction, f_{ebs}, for a given domain is defined as the ratio of backstreaming electron current, I_{ebs}, to the outgoing ion current, I_i, such that

$$f_{ebs} \equiv \frac{I_{ebs}}{I_i} \tag{5}$$

During experimental efforts, this ratio is used to describe the backstreaming fraction for the entire beam by comparing the total beam current to the total EBS current. The value of this parameter is found by continually

decreasing the magnitude of the accel grid voltage until a sharp rise in "measured" beam current indicates the beginning of prodigious electron backstreaming due to a decrease in the strength of the retarding potential near the accel grid apertures. As mentioned earlier, the onset of EBS is typically defined as the point where $f_{ebs} \sim 1\%$ for the entire beam. The computational method used by CEX2D-tebs for determining the $|V_{ebs}|$ mimics the experimental technique by incrementally lowering the magnitude of the accel grid voltage until a specified value of f_{ebs} for the entire grid or for certain gridlets is exceeded. This method is attractive from a computational perspective since each new value of accel grid voltage uses the potential solution from the previous accel grid voltage to provide relatively fast potential solution convergence.

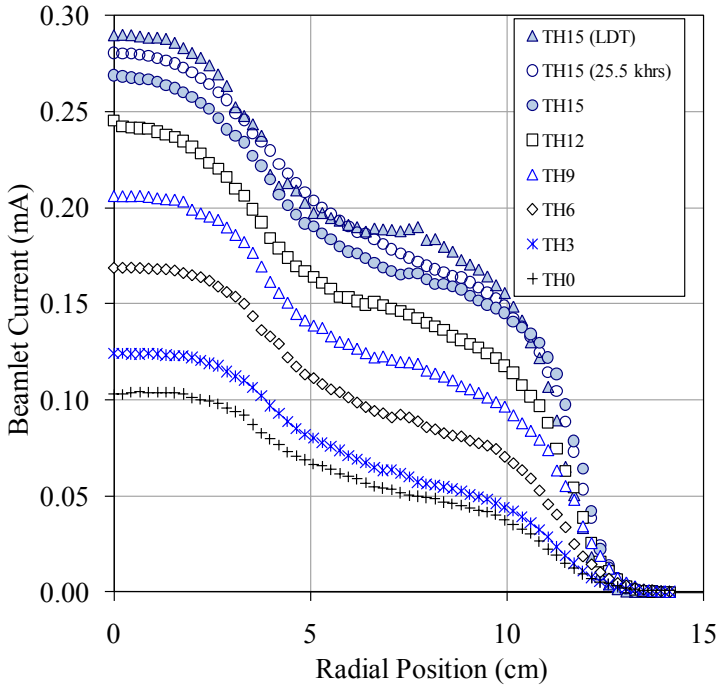

Figure 3. Beamlet current vs. radial position for the NSTAR ELT at various throttle conditions. Also shown is the profile at the beginning of the NSTAR LDT.

III. Results

This section uses the CEX2D-tebs model described above to examine the electron backstreaming for individual gridlets and across the beam of the NSTAR thruster for the conditions used during the LDT and ELT experiments.

A. Inputs for Ion Optics Erosion and EBS Analysis

Results from long-duration testing of the NSTAR thrusters showed that the center region of the grids experienced the significant erosion and accel grid aperture enlargement [1,2,7]. Preliminary computational analysis showed that these features lead to increased electron backstreaming [3,5]. As discussed below, the erosion and $|V_{ebs}|$ analysis is primarily conducted at the center gridlet/beamlet since the highest beamlet current, most significant erosion, and smallest grid gap occur in the center region of the NSTAR grids [8]. As a result, the most significant changes to grid geometry and electron backstreaming occur in this region, thus dictating the $|V_{ebs}|$ trend for the entire grid.

Input parameters used for the model were derived from experimental and computational results [1,2,5,6,7]. The beamlet currents used for the analysis below are shown in Figure 3. This figure also provides the NSTAR beamlet profiles for the full range of throttle conditions (TH0 – TH15) at the beginning of the ELT, for TH15 near the end of the ELT (25.5 khrs), and for the NSTAR 8200-hour LDT. The potential for the downstream beam plasma, ϕ_{bp}, and electron temperature, T_e, were nominally 10 V and 1.8 eV. The upstream electron temperatures and and neutral densities for TH15 were taken from the values found by the ion thruster discharge chamber model, DC-ION, in

reference [9]. The grid gap for two-grid ion thrusters using molybdenum ion optics, such as NSTAR, typically reduces due to the differential thermal expansion of the screen and accel grid [6,8]. Therefore, the nominal hot grid gap (during thruster operation) used for the center hole at beginning of thruster life (at TH15) was the 0.30 mm spacing measured for TH15 in reference [6] (this assumes an initial cold grid gap of 0.66 mm and a lessening of the grid gap by 0.36 mm during thruster operation). For lower throttle conditions, nominal values for changes in hot grid gap of approximately -0.35 and -0.20 mm for throttle conditions TH8 and TH0 were used [6]. Since data on the radial variation of the hot grid gap is unavailable, this study assumes that the hot grid gap varies linearly from the minimum at the center of the grid to the cold grid gap value at the grid periphery. Post-test analysis for the ELT showed that the cold grid gap had changed approximately -0.19 mm. Previous analyses discussed in reference [3] and sensitivity analyses given below show that reduction of hot grid gap may explain sharp rises in the magnitude of the electron backstreaming later in thruster life.

B. EBS determination

An example of $|V_{ebs}|$-curves generated by CEX2D-tebs for the NSTAR 8200-hour Long Duration Test (LDT) is shown in Figure 4 for a single gridlet using the method discussed in Section II using 1-volt increments in accel grid voltage. These data are similar to the $|V_{ebs}|$-curves used throughout this effort and are plotted on two ranges for the *y*-axis for clarity.

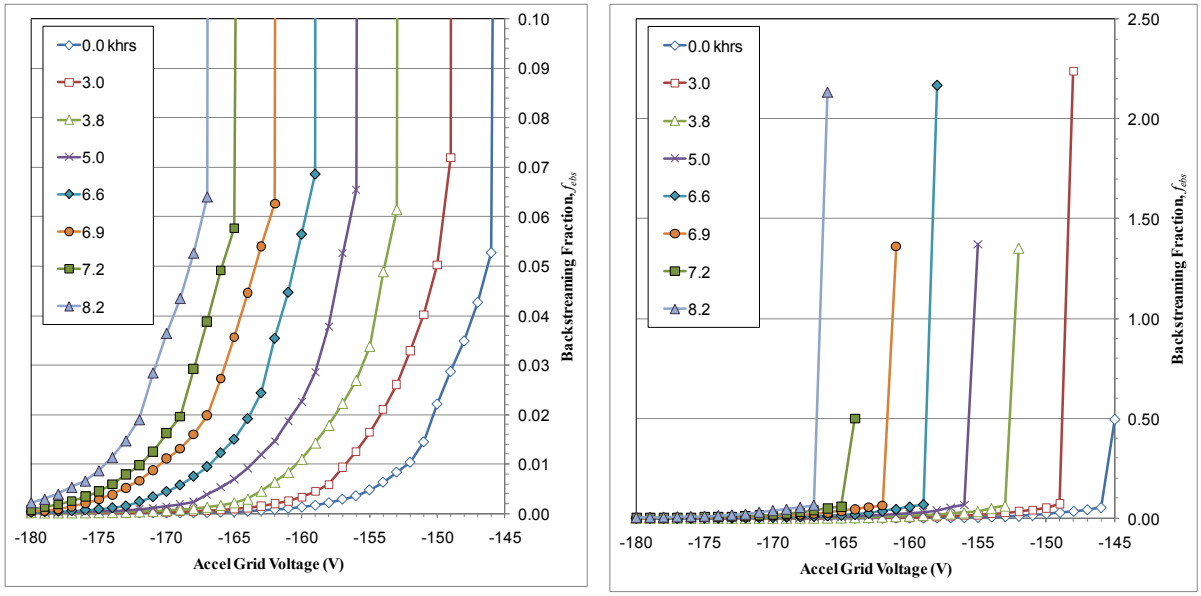

Figure 4. Typical $|V_{ebs}|$-curves for the NSTAR 8200 Long Duration Test for a single gridlet at different run times in khrs. These data are plotted on two different axes for f_{ebs} for clarity.

For NSTAR experiments, the fraction of electron backstreaming, f_{ebs}, for determining $|V_{ebs}|$ was set at 1%. In an effort to understand how the electron backstreaming varies over the radial extent of the grids, the CEX2D-tebs model was used to find f_{ebs} for several apertures along the NSTAR grid radius. For the beam profiles in Figure 3 it is reasonable to use trapezoidal integration between radii 0, 2, 4, 6, 8, 10, and 13 cm to determine the backstreaming limit for the entire beam. The "local f_{ebs}" values at these radial locations are given in Figure 5 for the condition where f_{ebs} = 1% for the entire beam. In general, for the NSTAR beam profiles at all throttle conditions it was found that a *local* value of $f_{ebs} \approx 10\%$ for the center hole corresponds to a "total f_{ebs}" of 1% for the entire beam. It was also found that over 99% of the backstreaming current occurs inside of r = 6 cm of the over 28 cm diameter NSTAR grids. Based on these results, an electron backstreaming limit condition of $f_{ebs} \approx 10\%$ for the center gridlet was used in the following analyses. Inspection of the nearly vertical shape of the $|V_{ebs}|$-curves above 10% (such as those in Figure 4) reveals that specifying this condition anywhere above 10% will change the $|V_{ebs}|$ result by only about one volt or less.

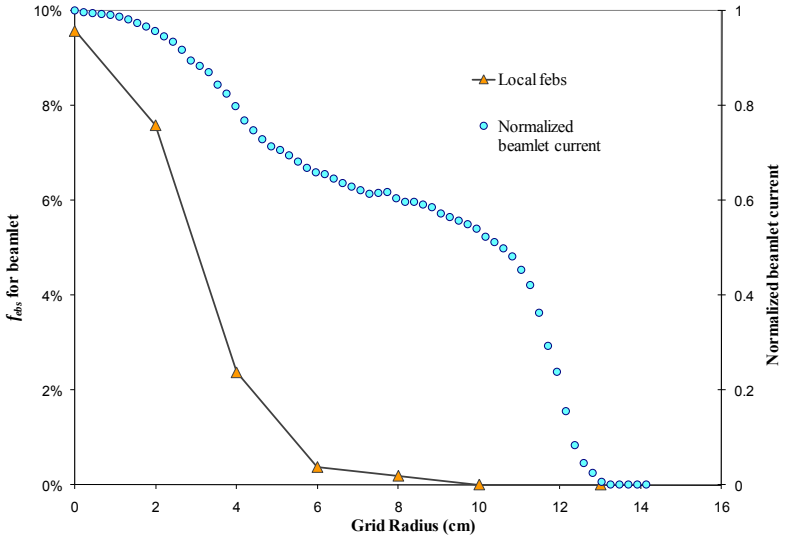

Figure 5. Local f_{ebs} values across a normalized NSTAR beam.

C. Comparison of CEX2D-tebs results with LDT data

Using the method discussed above, the CEX2D-tebs model was run for the conditions during the NSTAR LDT and ELT long duration tests. For the LDT, the model was run at TH15 for 8200 hours at the conditions described in [2] and discussed above. The trend of $|V_{ebs}|$ values vs. runtime are compared to the LDT data in Figure 6 and show good agreement for a grid gap of l_g = 0.30 mm. Improved agreement is found for a grid gap of l_g = 0.34 mm. This gap is reasonable since the NSTAR LDT thruster is not the same thruster as the NSTAR engineering model used for the measurements in reference [6]. Therefore, it is possible that the grid gap for the two thrusters differs by 40 microns, a difference of about 13%. An interesting trend that is evident in this plot is that, for these conditions, the larger grid gap starts at a lower $|V_{ebs}|$ but causes a steeper rise in magnitude. By examining the erosion rates for the conditions in Figure 6, it is clear that the larger grid gap results in slightly faster erosion of the accel grid aperture, thus leading to the different rate of change in $|V_{ebs}|$ shown in the plot.

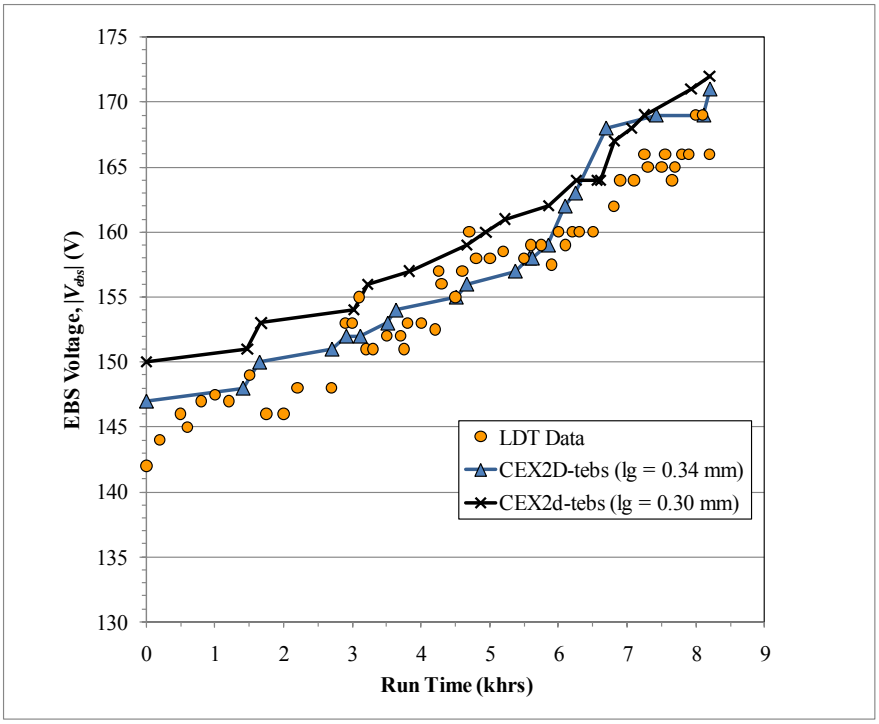

Figure 6. CEX2D-tebs results compared to LDT Data for two different grid gap, l_g, values.

D. Comparison of CEX2D-tebs results with ELT data

One of the major advantages of CEX2D-tebs is the ability to allow the user to specify the grid gap at any time during the thruster operation. Changes in grid gap can be caused by different operating conditions or changes due to grid erosion [3,6,8]. During the NSTAR ELT, the thruster was run at multiple throttle levels during the over 30 khrs of operation. During this test, the grids experienced significant erosion and a decrease in the cold grid gap was measured during post-test analysis [7]. As discussed in reference [3], a decrease in grid gap helps explain the $|V_{ebs}|$ trends observed during the NSTAR ELT. As a result, a few different trends in grid gap were analyzed to examine the effect of decreasing grid gap on the accuracy of $|V_{ebs}|$ values in comparison to ELT data. By comparing the grid gaps from Table 1 and the corresponding CEX2D-tebs results in Figure 7, it is clear that good agreement can be achieved if a decreasing grid gap is considered. Comparing the results from Run 1 and Run 2 shows that if the grid gap at the beginning of the test is 0.34 mm instead of 0.30 mm, similar to the LDT results, some improved agreement with the data during later Test Segments is found. The best agreement with end of test and maximum $|V_{ebs}|$ (which can signify end of thruster life) occurs with a gradual change in the grid gap for TH15 as shown in Run 3; however this scenario does not reproduce the sharp rise seen during Test Segment 5. The results shown here specify a constant grid gap during each Test Segment. As discussed below, future efforts will investigate the possibility of gradual grid gap changes during each Test Segment.

Table 1. Input Sets (Run 1, Run 2, and Run 3) for ELT Simulations

Test Segment	Throttle Level	Grid Gap (mm)		
		Run 1	Run 2	Run 3
1	TH15	0.30	0.34	0.34
2	TH8	0.34	0.34	0.34
3	TH15	0.25	0.25	0.3
4	TH0	0.45	0.45	0.45
5	TH15	0.25	0.25	0.25
6	TH5	0.25	0.25	0.25

These data also include an increase in beamlet current at the center gridlet over the life of the test for TH15 of about 4.5% after 25.5 khrs, as shown in Figure 3. The increase in beamlet current was assumed to grow gradual over the life of the test to the value given for the TH15 condition at 25.5 khrs. To show the effects of including increasing beamlet current, "Run 4" was conducted with the same conditions as Run 1, except *without* increasing beam current. A comparison of Run 1 and Run 4 in Figure 8 shows that increasing beamlet current helps capture the steep rise in $|V_{ebs}|$ during Test Segment 5 and the $|V_{ebs}|$ values during Test Segment 6.

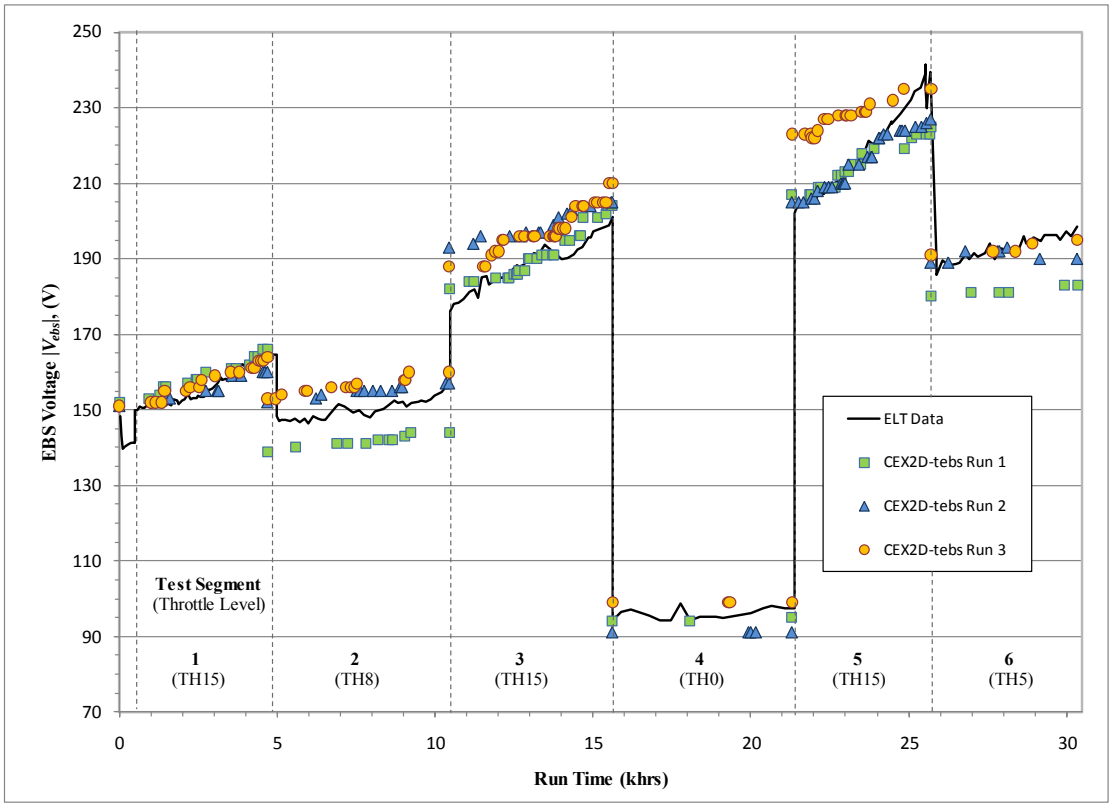

Figure 7. Comparison of CEX2D-tebs results for Runs 1, 2, and 3 with data from ELT.

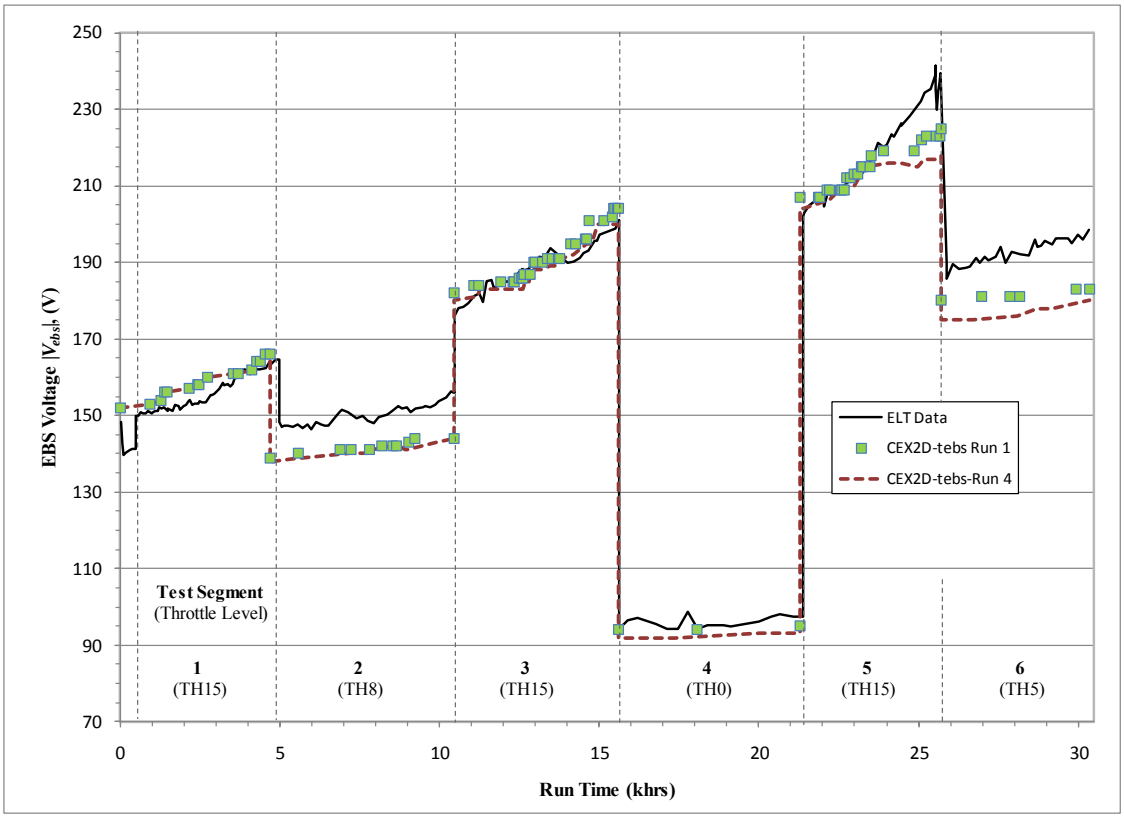

Figure 8. Comparison of CEX2D-tebs results for changing beamlet current. Run 4 is identical to Run 1, except without increasing nominal beamlet current during the test.

IV. Conclusions

The results from this paper show that CEX2D-tebs provides useful and accurate assessments of long duration electron backstreaming for ion optics. By integrating electron backstreaming current over the thruster beam it was found that over 99% of the backstreaming current occurs inside of r = 6 cm for the over 28 cm diameter NSTAR grid. Additionally, a value of f_{ebs} = 10% for the center gridlet corresponded to $f_{ebs} \sim 1\%$ over the entire beam. Consequently, a nominal value of f_{ebs} = 10% was used for the center gridlet to reflect $f_{ebs} \sim 1\%$ for the entire thruster. Analysis of the $|V_{ebs}|$-curves suggests that any reasonable value above 10% for the center gridlet should will change the $|V_{ebs}|$ by only about one volt. The CEX2D-tebs model agrees well with $|V_{ebs}|$ data from the long duration NSTAR tests, LDT and ELT. The best agreement for the LDT and ELT was found for an initial grid gap slightly larger than that measured in experimental test. The results further substantiate claims from previous analysis that suggests that decreasing grid gap, in addition to grid erosion, largely explains the steep rises in $|V_{ebs}|$ observed during the NSTAR ELT. Improved agreement with the ELT results is also found by including the effects of increasing center beamlet current with time, as was observed during thruster testing.

This work will be followed by additional analysis for long duration ion optics operation. These efforts will resolve electron backstreaming across the entire beam for the full duration of the tests. This effort will include self-consistent grid gap analysis, which will require improved understanding of grid gap changes over time at all radial locations. For this, initial efforts will be focused on the effects of differential thermal expansion of the grids due to grid erosion over the life of the thruster [10]. For grid erosion, additional work is needed to understand the impact of carbon deposition on the erosion rates of ion optics operated in ground tests. Other future efforts will include comparison with perveance and screen grid transparency data from ion thruster tests, and may include analysis of the tolerance a thruster may have to the formation of large "rogue holes" in the accel grid.

Acknowledgments

The author would like to thank Jun Araki from UCLA and John Anderson and John Brophy from JPL for the many thoughtful discussions and help with during the development of this task.

References

[1] Brophy J. R., "Propellant Throughput Capability of the DAWN Ion Thrusters," IEPC-2007-279.

[2] Polk J. E., et al, "An Overview of the Results from an 8200 Hour Wear Test of the NSTAR Ion Thruster," AIAA-99-2446, 35th AIAA/ASME/SAE/ASEE Joint Propulsion Conference and Exhibit, 20-24 June 1999, Los Angeles, California

[3] Wirz R., Katz I., Goebel D., Anderson J., "Electron Backstreaming Determination for Ion Thrusters," AIAA-2008-4732

[4] Brophy J. R., Katz I., Polk J., Anderson J. R., "Numerical Simulations of Ion Thruster Accelerator Grid Erosion," AIAA 2002-4261

[5] Wirz R., Anderson J., Katz I., Goebel D., "Time-Dependent Erosion of Ion Optics," AIAA-2008-4529

[6] Diaz E. M., Soulas G. C., "Grid Gap Measurement for an NSTAR Ion Thruster," NASA/TM-2006-214249, IEPC-2005-244.

[7] Anderson J. R., et al, "Post-Test Analysis of the Deep Space One Spare Flight Thruster Ion Optics," AIAA 2004-3610.

[8] Soulas G. C., "Calculation of Thermally-Induced Displacements in Spherically Domed Ion Engine Grids," IEPC-2005-248, *Presented at the 29th International Electric Propulsion Conference, Princeton University, October 31 – November 4, 2005*

[9] Wirz R., Katz I., "Plasma Processes of DC Ion Thruster Discharge Chambers," AIAA 2005-3690, *41st Joint Propulsion Conference*, Tucson, AZ, 2005

[10] Anderson J. R., et al, "Thermal Development Test of the NEXT PM1 Ion Engine," AIAA-2007-1803